Investigation of Gravity Wave-Driven Ionospheric Disturbances Using High-Resolution WACCM-X: A Machine Learning Framework for Wave Detection and Vertical Tracking

Sreelekshmi Radhakrishnan Girijakumary[1], Xian Lu[1], Clemson University

Abstract

Atmospheric gravity waves (AGWs) play a key role in coupling the lower atmosphere to the ionosphere-thermosphere (IT) system. In a recent AWE-GNSS observational study, nearly 65% of observed ionospheric disturbances were associated with mesospheric GWs, providing strong evidence of mesosphere-ionosphere coupling. However, observations alone cannot continuously track wave propagation across atmospheric layers. Here, we use the High-Resolution WACCM-X Nature Run and a machine-learning-based detection framework to identify and track GWs from the lower atmosphere to ionospheric heights. By linking detected wave packets to ionospheric disturbances, we classify events as Primary GW-driven, Secondary GW-driven, or Non-GW and compute coupling fractions by season, latitude, and local time. Results show that 54% of detected disturbances are directly linked to GWs propagating from the lower atmosphere. Coupling is strongest at mid-to-high latitudes and during post-midnight to morning local times.

Background

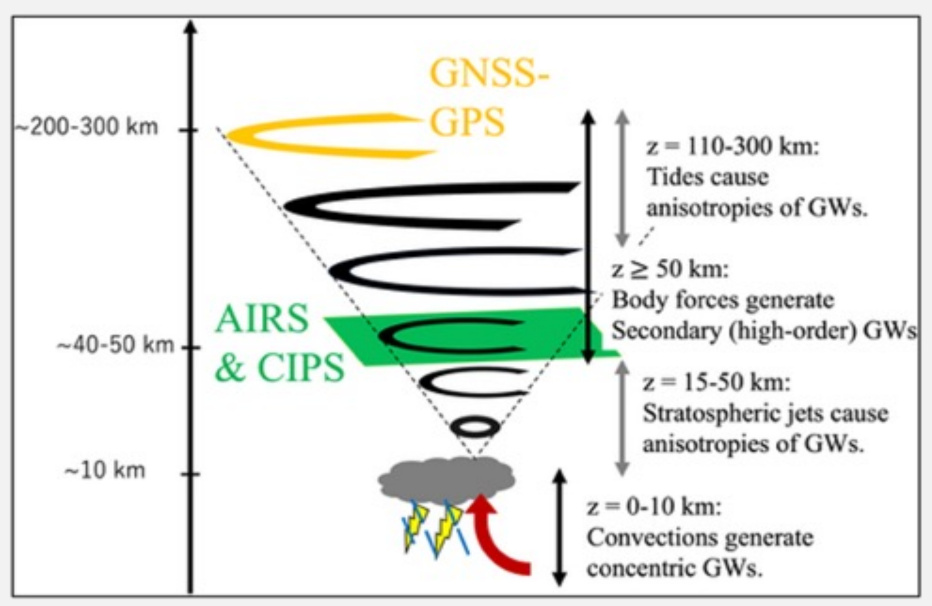

Fig 1. Schematic illustration of upward propagating AGWs generating TIDs (Kogure et al, 2025).

Electron-density modulations (MSTIDs)
↑
Ion-neutral collisions
↑
GWs perturb neutral winds
↑
Tropospheric weather

AWE-GNSS observational evidence of mesosphere-ionosphere coupling

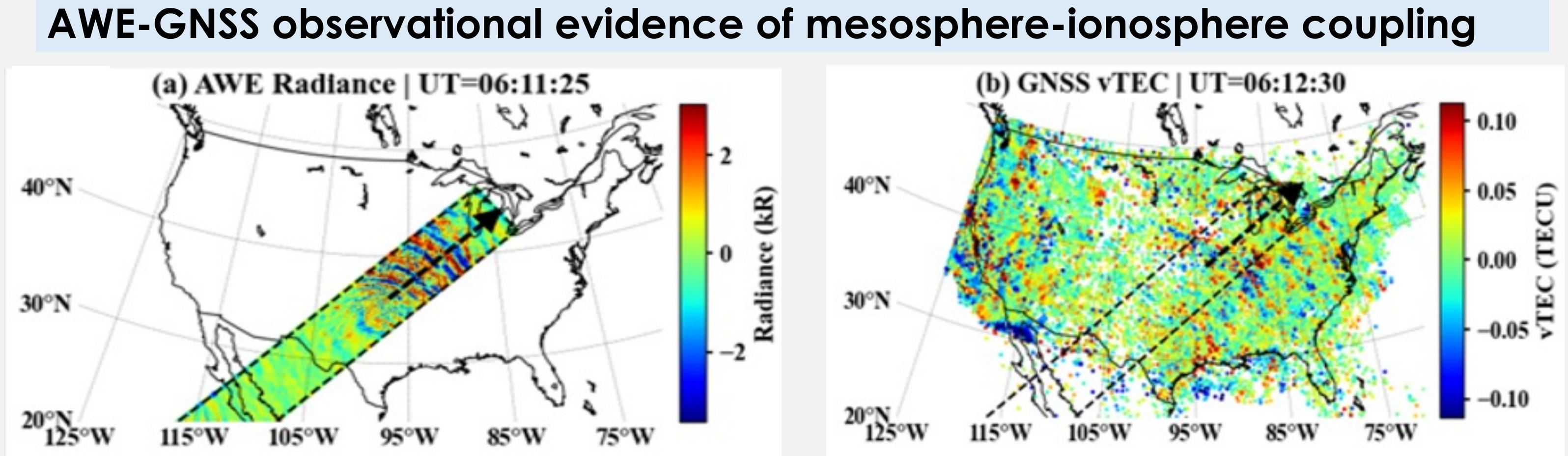

Fig 2. Coordinated AWE (87 km) radiance and GNSS (300 km) vTEC observations revealing coherent mesospheric and ionospheric wave structures (Girijakumary and Lu, GRL 2026, under review).

Motivation

Observations alone cannot continuously track vertical gravity wave propagation, making it challenging to distinguish GW-driven ionospheric disturbances from locally generated plasma instabilities.

Science Questions

1. **What fraction of ionospheric disturbances can be attributed to GWs propagating upward from the lower atmosphere?**
2. **How does GW-ionosphere coupling efficiency vary with latitude, local time, and season?**

Objectives

Develop an automated wave-packet detection and vertical tracking framework to quantify GW-driven ionospheric disturbances and their seasonal, latitudinal, and local-time dependence.

Model Used:

High-Resolution WACCM-X Nature Run (NE120/L273), a whole-atmosphere simulation extending from the surface to ~ 600 km with ~25 km horizontal resolution.

Methodology Workflow

1. 2-D FFT Spectral Filtering

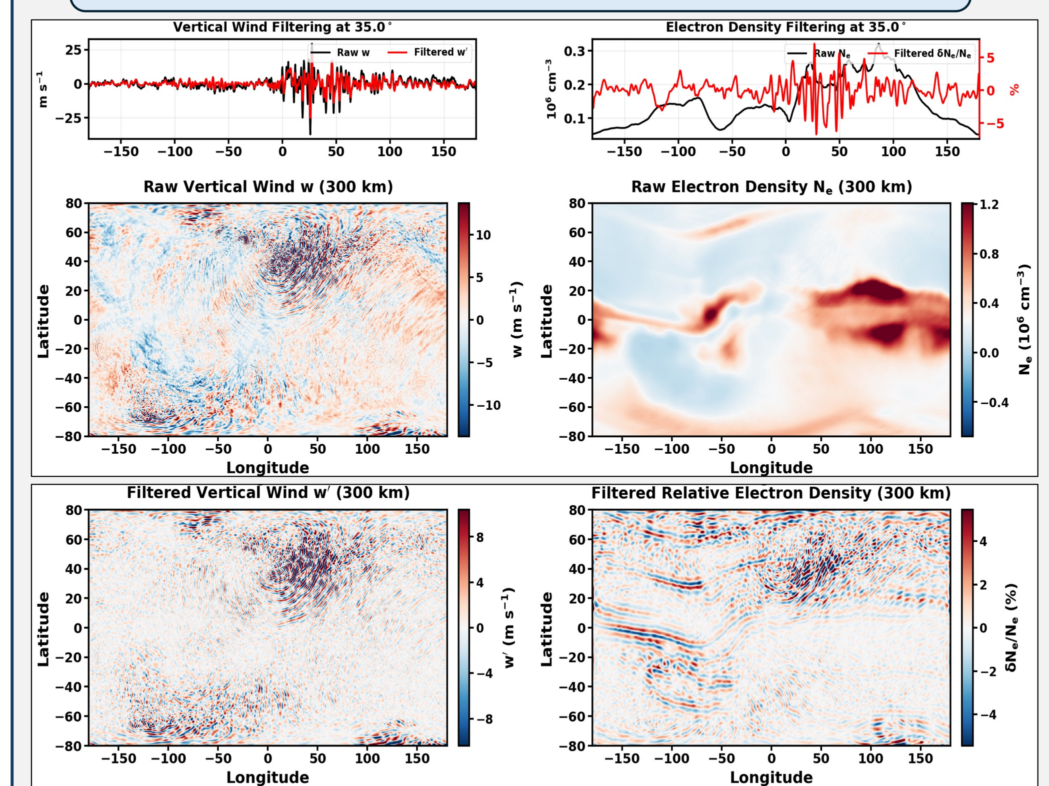

Fig. 3. 2-D FFT filtering of vertical wind and electron density fields used to isolate medium-scale GWs and ionospheric perturbations (200–1000 km).

2. Training Dataset

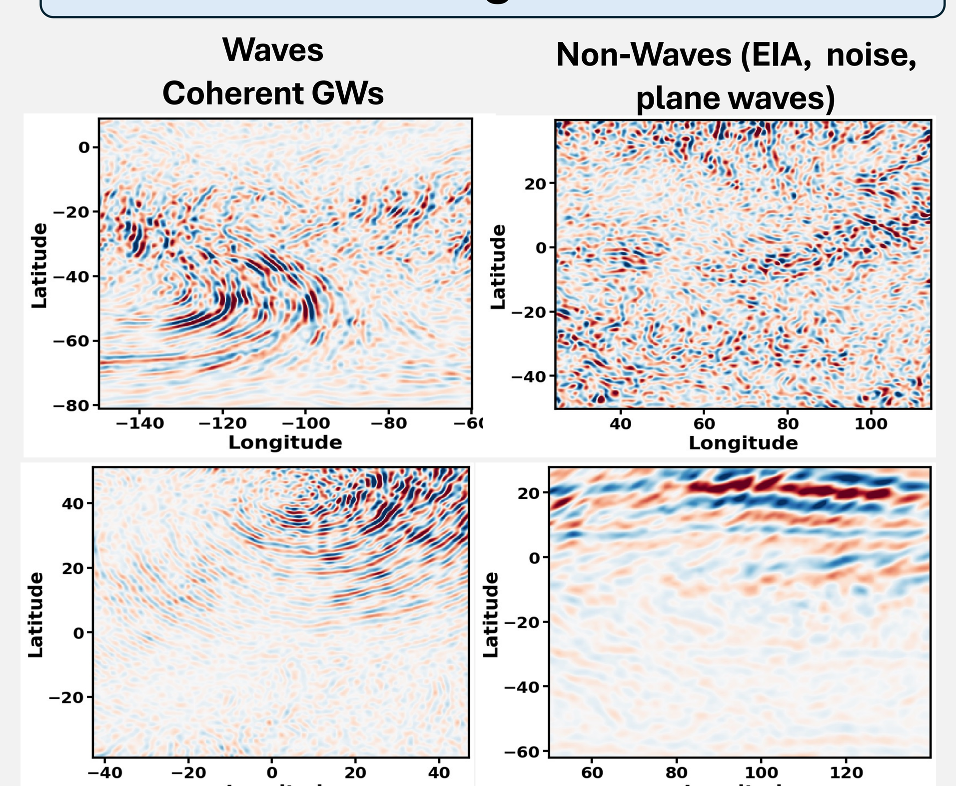

Fig. 4. Manually labeled wave (N=300) and non-wave (N=300) patches used for Random Forest training.

3. Feature extraction

(Amplitude, circularity, radial & spectral structure)

4. Random Forest Training

(Learn distinguishing wave-packet characteristics from labeled examples)

5. Variance-Based Candidate Detection

High wave-energy regions are selected as candidate wave packets.

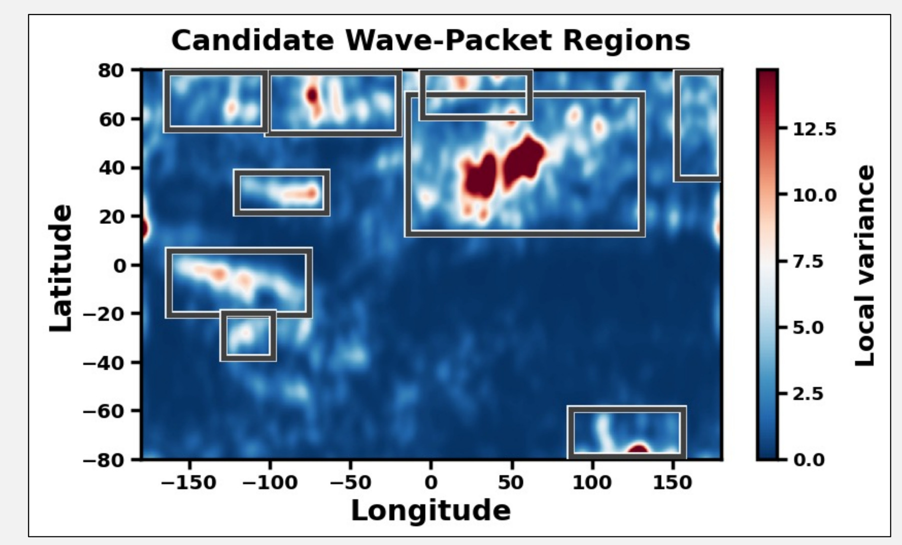

Fig. 5. Variance-based identification of candidate wave-packet regions.

6. RF Classification of Candidates

High variance identifies candidate regions, while the Random Forest determines whether the structure represents a coherent GW packet.

7. Final Wave-Packet Detection

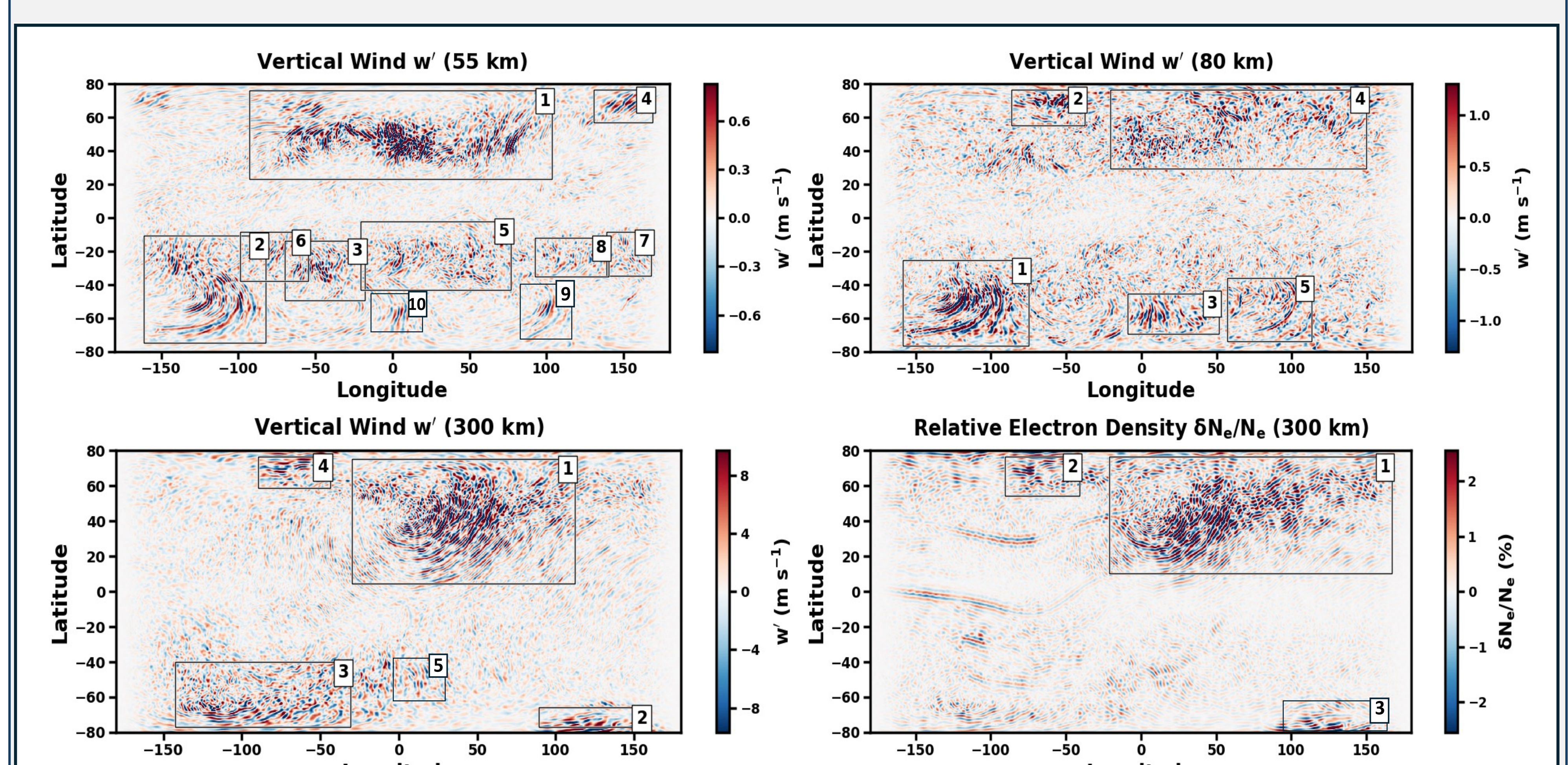

Fig. 6. Automated detection of coherent GW packets in filtered vertical wind perturbations and associated ionospheric disturbances in relative electron density at 300 km. Detected wave packets are linked across altitude levels, with an expanded spatial search window applied to account for horizontal displacement during upward propagation

Results

Detected GW and ionospheric wave packets are classified based on the vertical continuity of GW signatures

Primary GW-driven	Secondary GW-driven	Non-GW
• Tracked from lower-atmosphere to ionosphere • Lower atmospheric forcing	• Detected near ionospheric heights. • wave breaking, instabilities, wave-wave interactions)	• No associated GW detected • Instability-driven disturbance

Computed for representative seasonal months (Dec, Mar, July, and Oct) to quantify the occurrence of Primary GW-driven, Secondary GW-driven, and Non-GW disturbances.

$$\text{Coupling Fraction (\%)} = \frac{N_{\text{Primary,Secondary,or NonGW}}}{N_{\text{Total Disturbances}}} \times 100$$

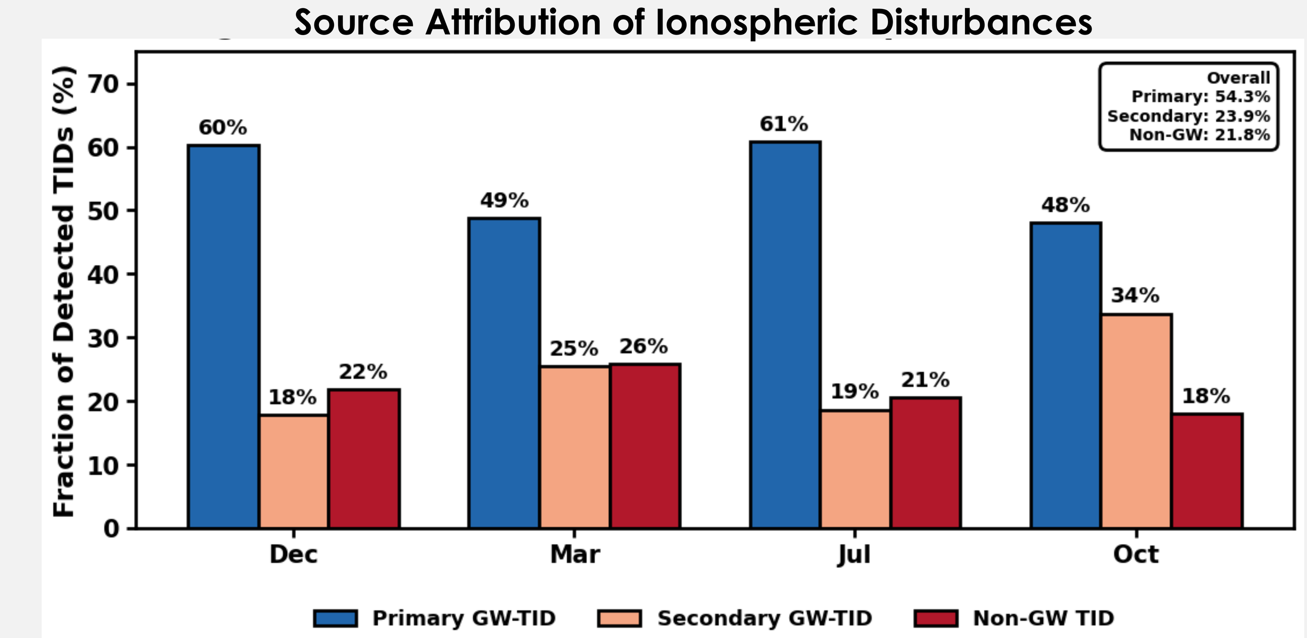

Fig. 7. Percentage of detected TIDs classified as Primary GW-driven, Secondary GW-driven, and Non-GW events for each season.

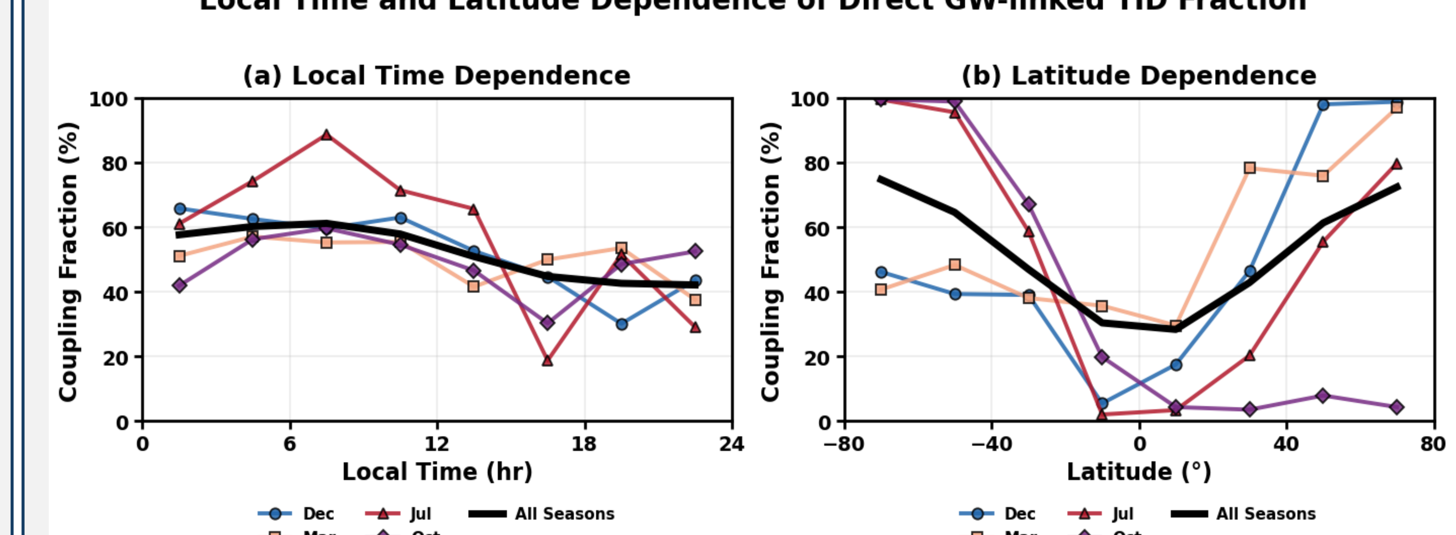

Fig. 8. Fraction of ionospheric disturbances classified as Primary GW-driven as a function of (a) local time and (b) latitude for each season and the all-season mean (black line).

Conclusions

- Within the 200-1000 km horizontal wavelength range examined here, ~54% of detected ionospheric disturbances are linked to GWs traced from the lower atmosphere.
- This fraction shows seasonal variability, reaching ~61% in July and ~60% in Dec.
- Direct GW coupling is strongest at mid-high latitudes, where over 60% of disturbances are GW-driven, consistent with the ~65% coupling fraction reported from AWE-GNSS observations over CONUS under quiet conditions.
- Primary GW-driven disturbances occur most frequently during post-midnight to morning hours, peaking near 06-10 LT.

Future Work

- Use controlled WACCM-X simulations to identify the atmospheric factors governing GW transmission and vertical coupling, including background winds, tides, and wave filtering.
- Investigate the impact of geomagnetic activity and ionospheric electrodynamics on coupling efficiency.

This work is supported by NASA grants 80NSSC22K0018, 80NSSC22K1010, and NSF grants CEDAR-2431688, AGS-2149695, and AGS-1753214